

## Supporting Information

# Impact of Anion Architecture on the Physicochemical and Transport Properties of Hexamethylguanidinium-Based Sodium-Ion Electrolytes

*Lukasz Kufel<sup>a</sup>, Julia Debono<sup>a</sup>, Elene Sasieta-Barrutia<sup>a</sup>, Luke A. O'Dell<sup>a</sup>, Wladyslaw Wieczorek<sup>b</sup>,*

*Craig Forsyth<sup>c</sup>, Maria Forsyth<sup>a</sup>, Jennifer M. Pringle<sup>a\*</sup>.*

- a. Institute for Frontier Materials, Deakin University, Burwood, VIC 3125, Australia
- b. Department of Chemistry, Warsaw University of Technology, Noakowskiego 3, 00664  
Warsaw, Poland
- c. School of Chemistry, Monash University, Clayton, VIC 3800, Australia

## Synthesis

### Hexamethylguanidinium chloride, [HMG]Cl

[HMG]Cl was prepared following previously reported methods.<sup>1</sup> Dichloromethylene dimethylammonium chloride (13.30 g, 82 mmol) was dissolved in 50 mL of dry dichloromethane in a pre-dried flask, which was cooled in an ice-water bath. A solution of dimethylamine in THF (143 mL, 2 M) was then added dropwise to the chilled, stirred solution over the course of an hour under an argon atmosphere. The reaction mixture was subsequently stirred overnight at room temperature, during which it developed a light-yellow colour. The organic solvent was removed under vacuum. The resulting yellow product mixture was dissolved in a 1:1 mixture of isopropanol and acetone (100 mL) and stored in a freezer at -20 °C overnight to precipitate dimethylammonium chloride ((CH<sub>3</sub>)<sub>2</sub>NH<sub>2</sub>Cl) as a salt. This process was repeated three times to maximize the removal of (CH<sub>3</sub>)<sub>2</sub>NH<sub>2</sub>Cl. Finally, the organic solvent was removed under vacuum, and obtained product was used for further synthesis. The synthesis route was adapted from Yunis et al. and consisted of metathesis reaction between the [HMG]Cl and respective Na-salts, NaTCM and NaTDI.<sup>2</sup>

### Hexamethylguanidinium tricyanomethanide, [HMG][TCM]

A mixture of 6:1 ratio of [HMG]Cl:(CH<sub>3</sub>)<sub>2</sub>NH<sub>2</sub>Cl (2.50 g, 9.57 mmol) was dissolved in 10 mL of water. Sodium tricyanomethanide (1.11 g, 9.82 mmol) was separately dissolved in 10 mL of water. Upon mixing the above solutions, a yellow precipitate formed instantly. CH<sub>2</sub>Cl<sub>2</sub> (20 mL) was added and the solution was left to stir for one hour at room temperature. The organic layer was washed with water (6 x 20 mL). Further, the organic layer was removed in vacuo for 24 hours at 50 °C, leading to a yellow solid of [HMG][TCM] (1.18 g, 5.03 mmol, 53% yield). <sup>1</sup>H NMR (400 MHz, DMSO): δ 2.89 (s, 18H) ppm; <sup>13</sup>C NMR (400 MHz, DMSO): δ 162.8, 121.0, 39.9, 5.2 ppm, Figure S35 and S36. Chloride content in the product was determined with ICP-MS at 79.7 ppb.

### Hexamethylguanidinium 4,5-dicyano-2-(trifluoromethyl)imidazolide, [HMG][TDI]

A mixture of 6:1 ratio of [HMG]Cl:(CH<sub>3</sub>)<sub>2</sub>NH<sub>2</sub>Cl (2.05 g, 7.85 mmol) was dissolved in 10 mL of water. Sodium 4,5-dicyano-2-(trifluoromethyl)imidazolide (1.74 g, 8.32 mmol) was separately dissolved in 10 mL of water. Upon mixing the above solutions, a yellow precipitate formed instantly. CH<sub>2</sub>Cl<sub>2</sub> (20 mL) was added and the solution was left to stir for one hour at room temperature. The organic layer was washed with water (6 x 20 mL). The organic layer was removed in vacuo for 24 hours at 50 °C to obtain a yellow solid. The product was recrystallized in 20 ml acetonitrile, which resulted in acquiring a white solid of [HMG][TDI] (1.92 g, 5.81 mmol, 74% yield). <sup>1</sup>H NMR (400 MHz, DMSO): δ 2.89 (s, 18H) ppm; <sup>13</sup>C NMR (400 MHz, DMSO): δ 162.8, 121.0, 39.9, 5.2 ppm; <sup>19</sup>F NMR (400 MHz, DMSO): δ 62.2 ppm, Figure S37-S39. Chloride content in the product was determined with ICP-MS at 39.8 ppb.

Table S1. Comparison of melting temperatures ( $T_m$ ) and glass transition temperatures ( $T_g$ ) between materials with [TCM]<sup>-</sup> and [TDI]<sup>-</sup> anions paired with common cations.

	$T_m$ (°C) [ $\Delta S_f$ (J mol <sup>-1</sup> K <sup>-1</sup> )]				$T_g$ (°C)			
	[C <sub>2</sub> mpyr] <sup>+</sup>	[C <sub>4</sub> mpyr] <sub>+</sub>	[C <sub>2</sub> mlm] <sup>+</sup>	[C <sub>4</sub> mlm] <sup>+</sup>	[C <sub>2</sub> mpyr] <sub>+</sub>	[C <sub>4</sub> mpyr] <sub>+</sub>	[C <sub>2</sub> mlm] <sup>+</sup>	[C <sub>4</sub> mlm] <sup>+</sup>
[TCM] <sup>-</sup>	45 [15] <sup>3</sup>	-8 [24] <sup>3</sup> -1 [**] <sup>4</sup>	-10 [29] <sup>3</sup>	_* 4	_* 3	-92 <sup>3</sup>	-85 <sup>3</sup> -88 <sup>4</sup>	-78 <sup>4</sup>
[TDI] <sup>-</sup>	56 [34] <sup>5</sup>	49 [**] <sup>6</sup>	61 [158] <sup>7</sup>	_* 7	_* 5	_* 6	-98 <sup>7</sup>	-69 <sup>7</sup>

\*no crystallisation/glass transition observed

\*\*not reported

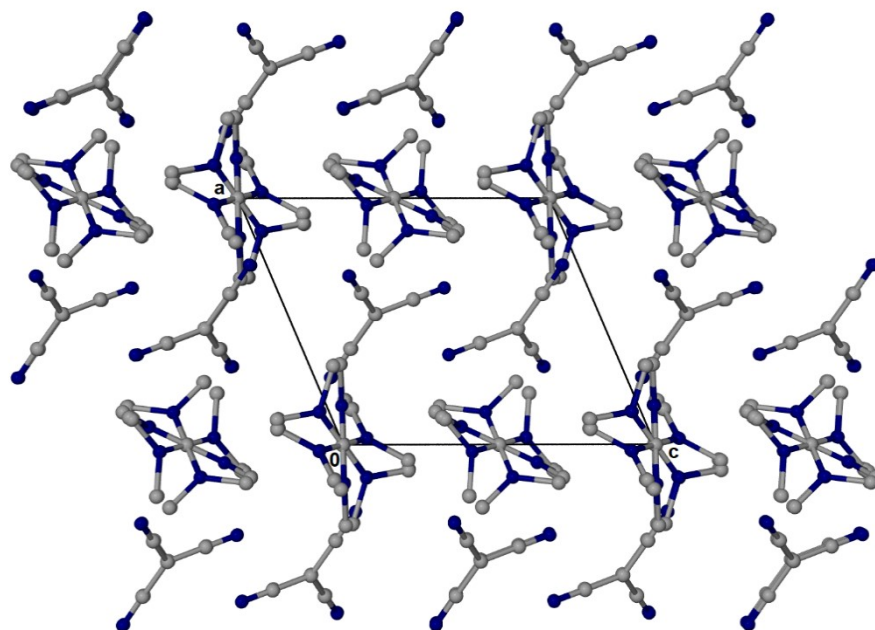


Figure S1. Cell packing in [HMG][TCM] crystal as viewed own the b axis; hydrogen atoms have been omitted for clarity.

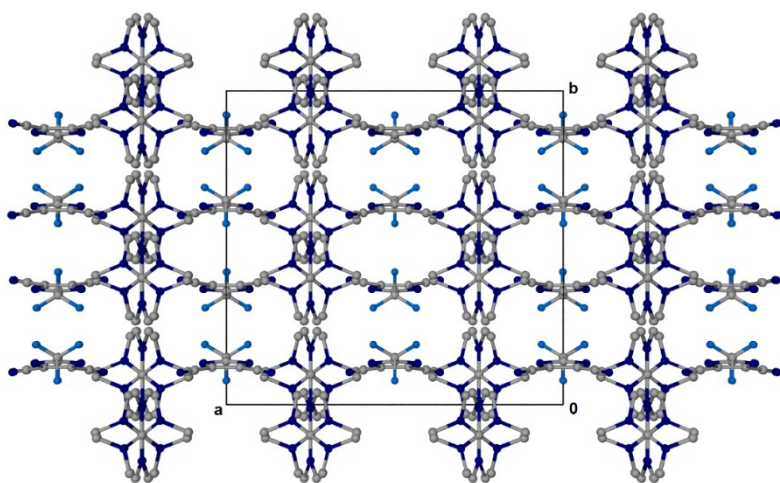
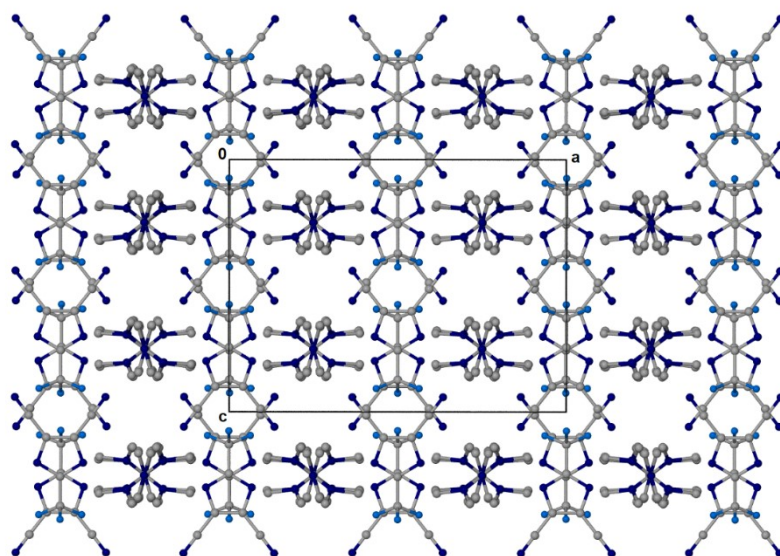


Figure S2. Cell packing in [HMG][TDI] crystal as viewed down the b (top) and c (bottom) axes.

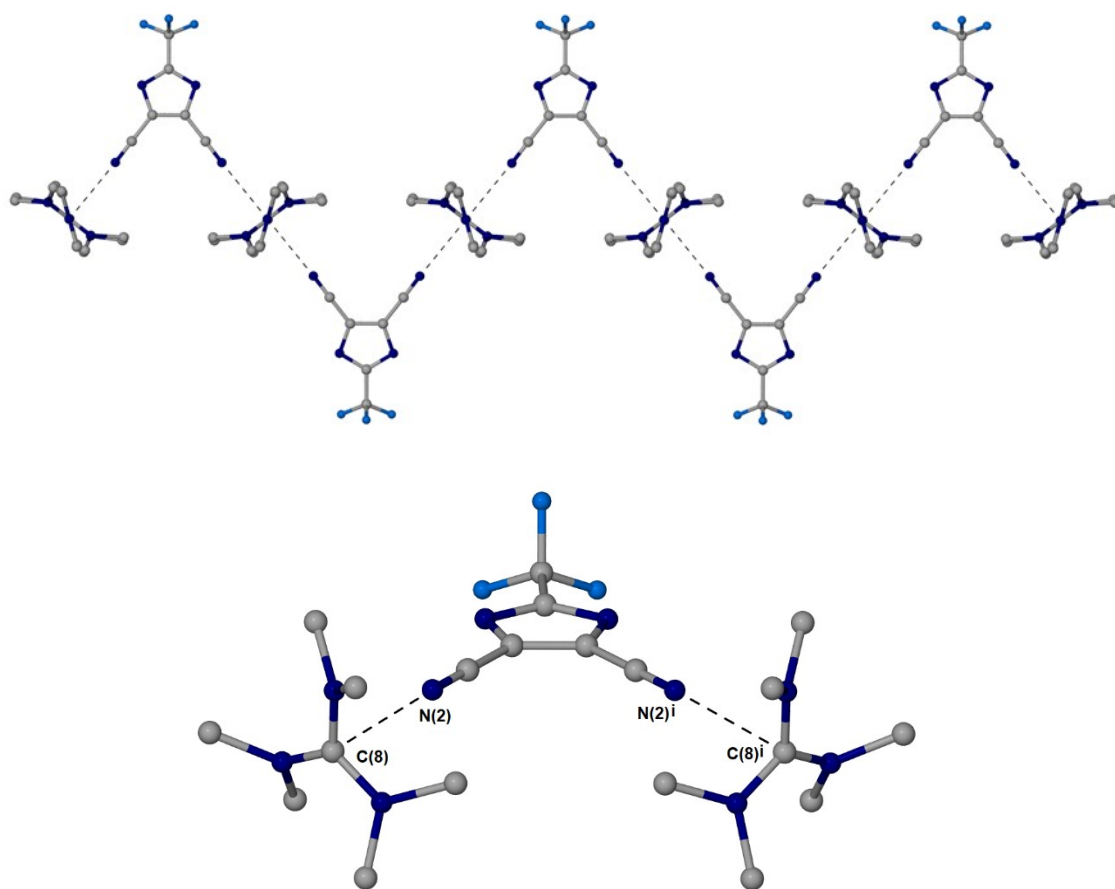


Figure S3. Zoom-in modelled position of the [TDI]<sup>-</sup> anion in [HMG][TDI] a crystal cell, demonstrating the CN groups positioning towards the central carbon atoms of the [HMG]<sup>+</sup> cation.

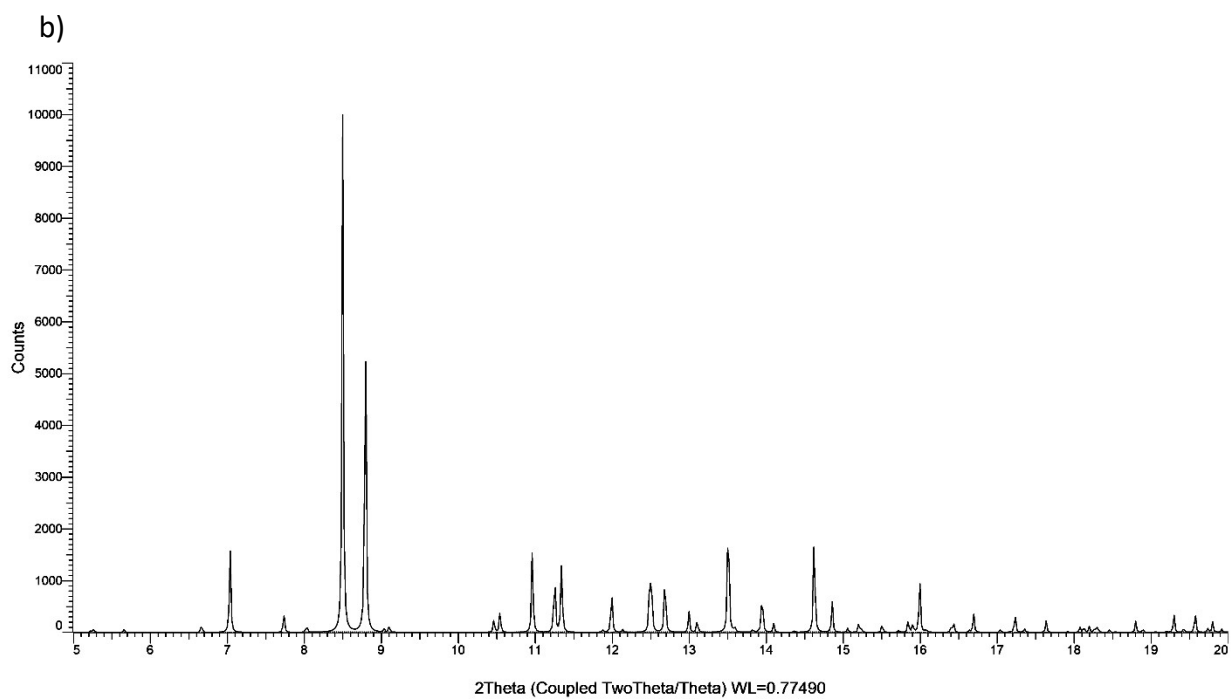
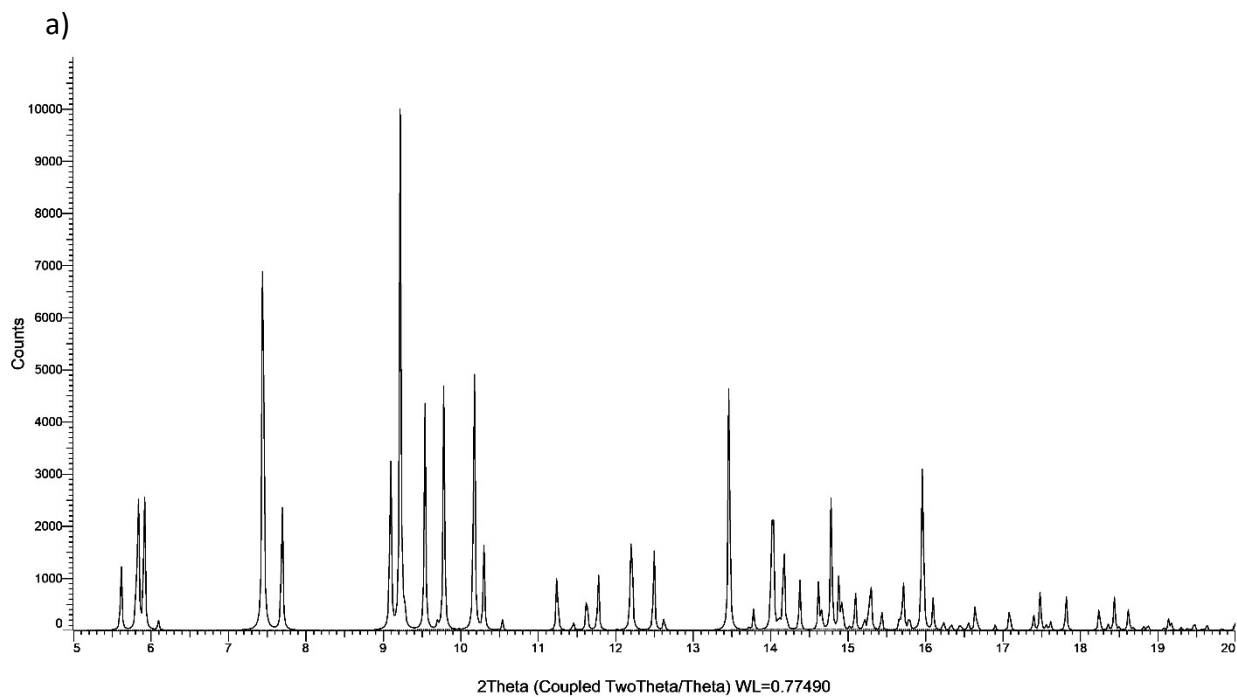


Figure S4. Powdered XRD patterns calculated from the crystal structures (a) [HMG][TDI] and (b) [HMG][TDI].

Table S2. Atomic coordinates ( $\times 10^4$ ) and equivalent isotropic displacement parameters ( $\text{Å}^2 \times 10^3$ ) for [HMG][TDI] U(eq) is defined as one third of the trace of the orthogonalized  $U_{ij}$  tensor.

	x	y	z	U (eq)
F (1)	5000	5771 (1)	9256 (1)	64 (1)
F (2)	4363 (1)	6918 (1)	9071 (1)	68 (1)
N (1)	4321 (1)	6320 (1)	7015 (1)	31 (1)
N (2)	3657 (1)	6036 (1)	4407 (1)	45 (1)
N (3)	2500	5117 (1)	2500	31 (1)
N (3')	2500	6787 (3)	2500	42 (1)
N (4)	3036 (1)	6392 (1)	1927 (1)	36 (1)
N (4')	1956 (2)	5508 (2)	3051 (3)	34 (1)
C (1)	5000	6388 (1)	7556 (1)	28 (1)
C (2)	4587 (1)	6199 (1)	6009 (1)	27 (1)
C (3)	4068 (1)	6109 (1)	5124 (1)	33 (1)
C (4)	2695 (3)	4617 (4)	1567 (5)	43 (1)
C (7)	5000	6510 (1)	8728 (1)	36 (1)
C (4')	2687 (10)	7332 (12)	1629 (14)	55 (3)
C (5)	3841 (6)	6053 (9)	1788 (10)	57 (2)
C (8)	2500	5958 (1)	2500	26 (1)
C (5')	2100 (8)	4702 (10)	3558 (12)	55 (4)
C (6)	2861 (5)	7176 (5)	1389 (6)	53 (1)
C (6')	1128 (15)	5880 (20)	3120 (30)	71 (7)

Table S3. Atomic coordinates ( $\times 10^4$ ) and equivalent isotropic displacement parameters ( $\text{Å}^2 \times 10^3$ ) for [HMG][TCM] crystal. U(eq) is defined as one third of the trace of the orthogonalized  $U_{ij}$  tensor.

	x	y	z	U (eq)
N (1)	8410 (2)	4903 (2)	9497 (2)	24 (1)
N (2)	10251 (2)	4268 (2)	10840 (2)	23 (1)
N (3)	11336 (2)	6120 (2)	9696 (2)	24 (1)
N (4)	1316 (2)	-483 (2)	5006 (1)	23 (1)
N (5)	-287 (2)	591 (2)	4039 (2)	24 (1)
N (6)	-724 (2)	-272 (2)	5969 (2)	24 (1)
N (7)	3162 (1)	3821 (1)	7498 (1)	41 (1)
N (8)	7278 (1)	9480 (1)	9479 (1)	47 (1)
N (9)	3646 (1)	6723 (1)	4615 (1)	56 (1)
C (1)	4706 (1)	6653 (1)	7182 (1)	30 (1)
C (2)	3869 (1)	5089 (1)	7346 (1)	31 (1)
C (3)	6112 (1)	8209 (1)	8450 (1)	32 (1)
C (4)	4116 (1)	6683 (1)	5766 (1)	37 (1)
C (10)	10000	5000	10000	24 (1)
C (11)	8210 (10)	6302 (12)	9340 (11)	31 (1)
C (12)	6740 (5)	3249 (4)	8996 (4)	31 (1)
C (13)	9357 (9)	3950 (11)	11868 (10)	26 (1)
C (14)	11434 (9)	3622 (12)	10757 (10)	30 (1)
C (15)	13197 (5)	7138 (4)	10771 (4)	29 (1)
C (16)	11025 (10)	6302 (11)	8250 (10)	28 (1)
C (20)	0	0	5000	26 (1)
C (21)	2535 (4)	-216 (4)	6396 (4)	32 (1)
C (22)	1537 (6)	-1195 (5)	3613 (4)	31 (1)
C (23)	1034 (9)	1678 (10)	3609 (8)	32 (2)
C (24)	-2082 (4)	201 (4)	3338 (4)	32 (1)
C (25)	-1330 (6)	865 (5)	6592 (5)	32 (1)
C (26)	-1112 (10)	-1689 (9)	6454 (9)	31 (2)

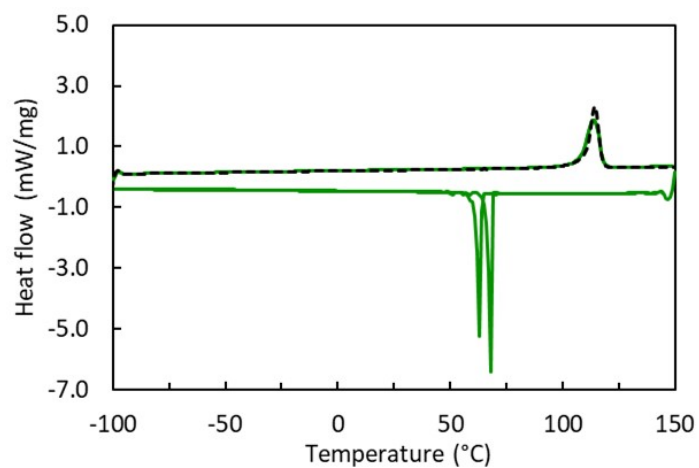


Figure S5. DSC curve of neat [HMG][TDI]. Scan rate: 10 K min<sup>-1</sup>

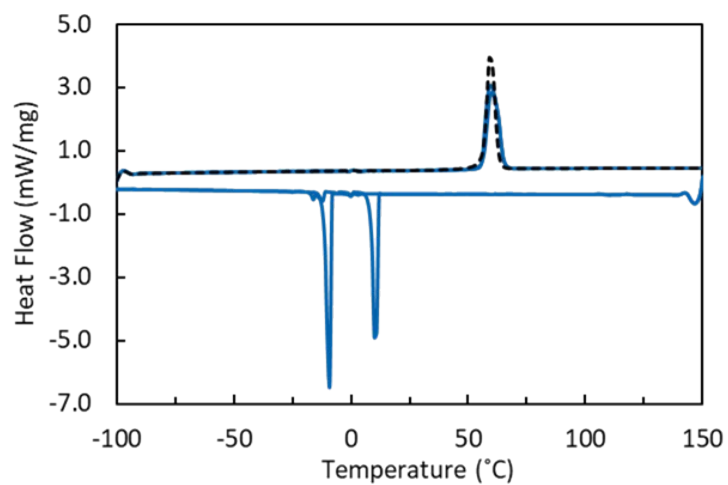


Figure S6. DSC curve of neat [HMG][TCM]. Scan rate: 10 K min<sup>-1</sup>.

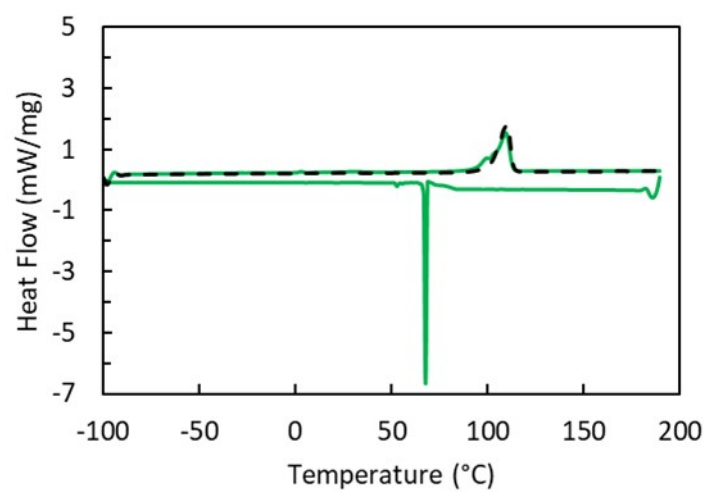


Figure S7. DSC curve of [HMG][TDI] + 5% NaTDI. Scan rate: 10 K min<sup>-1</sup>.

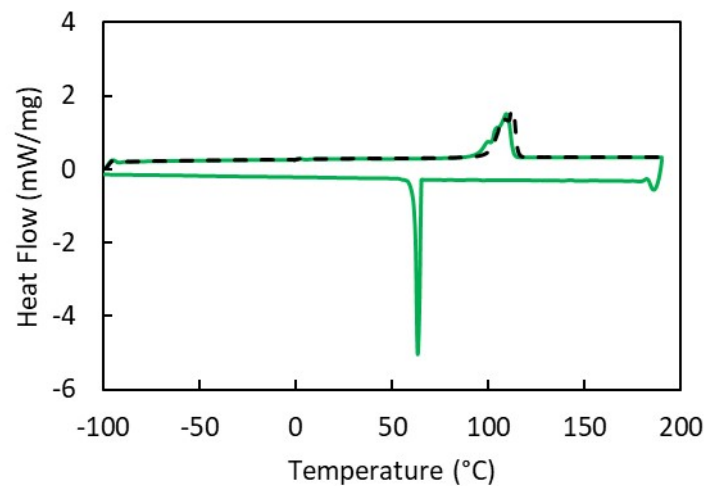


Figure S8. DSC curve of [HMG][TDI] + 10% NaTDI. Scan rate: 10 K min<sup>-1</sup>.

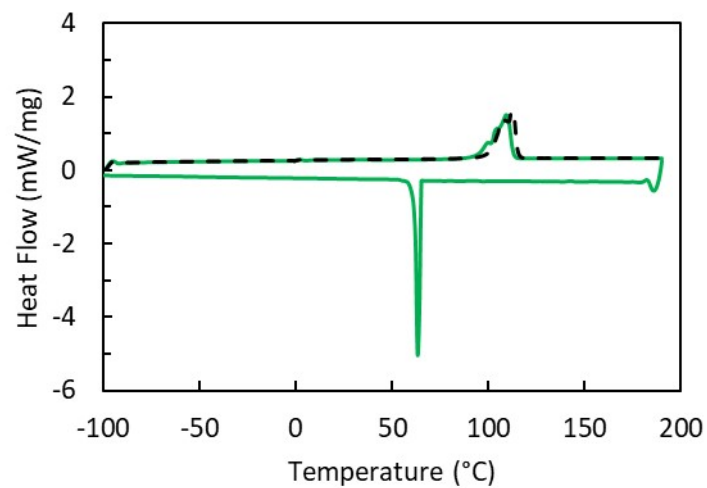


Figure S9. DSC curve of [HMG][TDI] + 15% NaTDI. Scan rate: 10 K min<sup>-1</sup>.

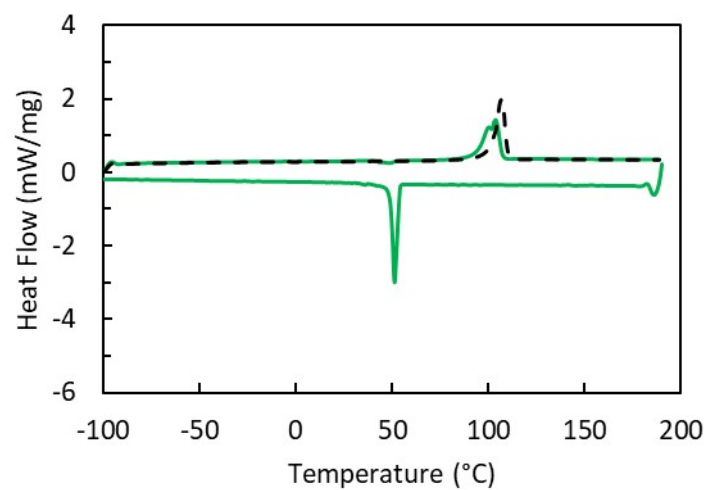


Figure S10. DSC curve of [HMG][TDI] + 20% NaTDI. Scan rate: 10 K min<sup>-1</sup>.

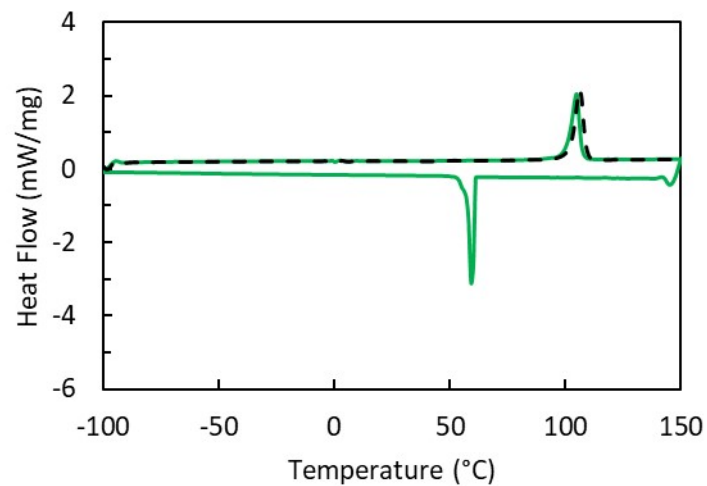


Figure S11. DSC curve of [HMG][TDI] + 30% NaTDI. Scan rate: 10 K min<sup>-1</sup>.

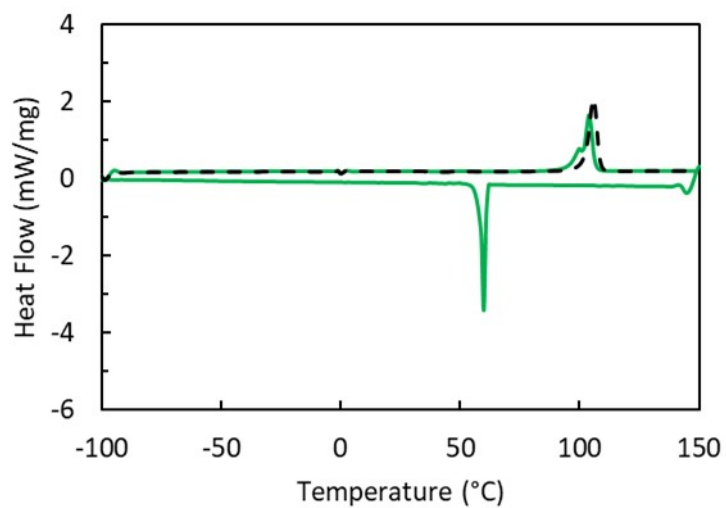


Figure S12. DSC curve of [HMG][TDI] + 40% NaTDI. Scan rate: 10 K min<sup>-1</sup>.

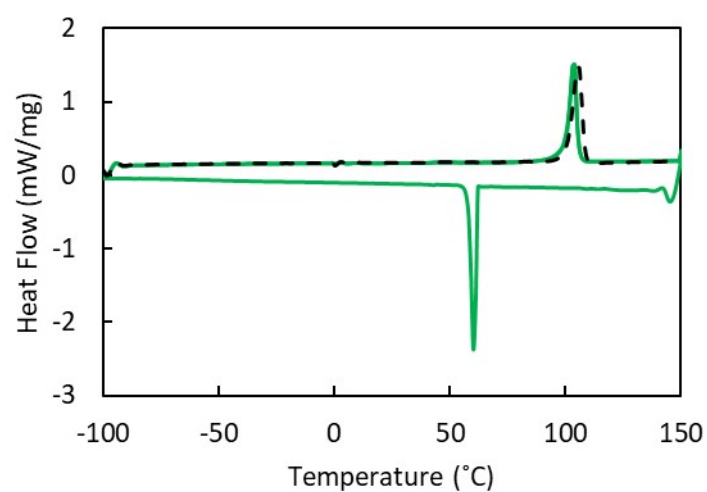


Figure S13. DSC curve of [HMG][TDI] + 50% NaTDI. Scan rate: 10 K min<sup>-1</sup>.

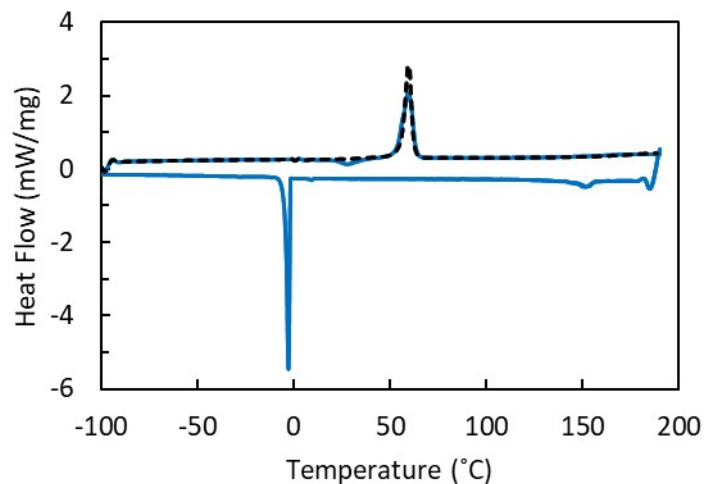


Figure S14. DSC curve of [HMG][TCM] + 10% NaTCM. Scan rate: 10 K min<sup>-1</sup>.

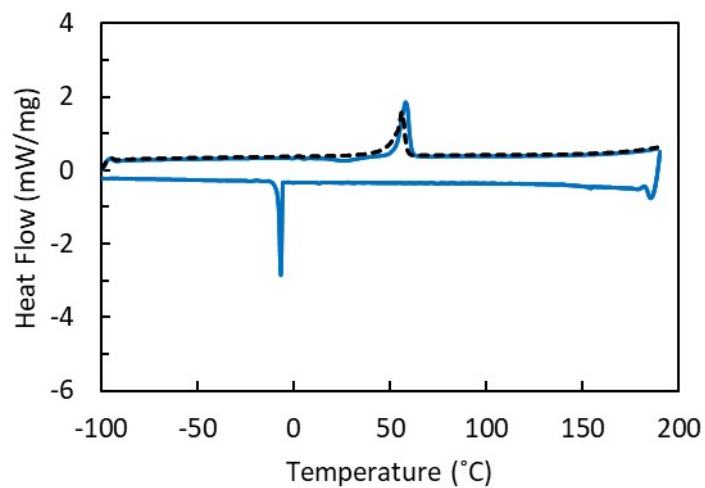


Figure S15. DSC curve of [HMG][TCM] + 20% NaTCM. Scan rate: 10 K min<sup>-1</sup>.

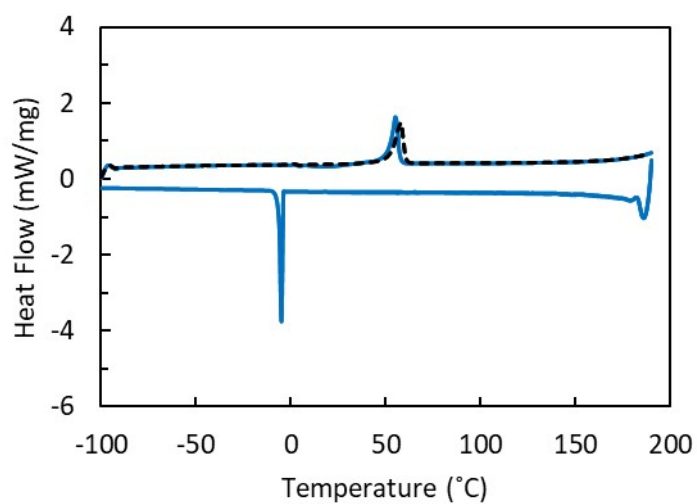


Figure S16. DSC curve of [HMG][TCM] + 30% NaTCM. Scan rate: 10 K min<sup>-1</sup>.

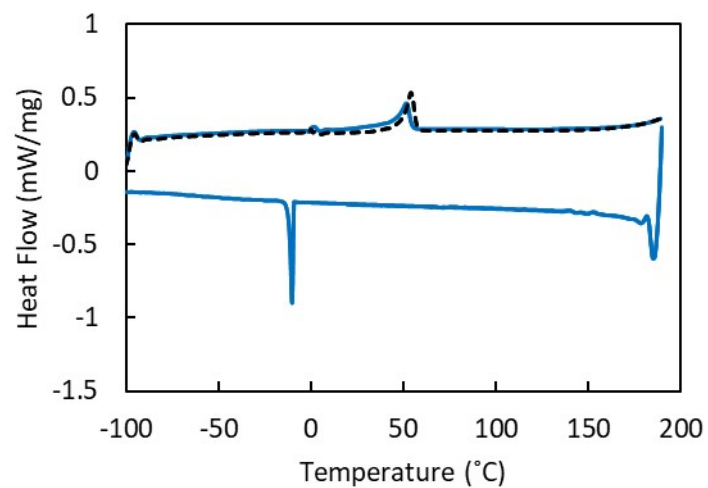


Figure S17. DSC curve of [HMG][TCM] + 40% NaTCM. Scan rate: 10 K min<sup>-1</sup>.

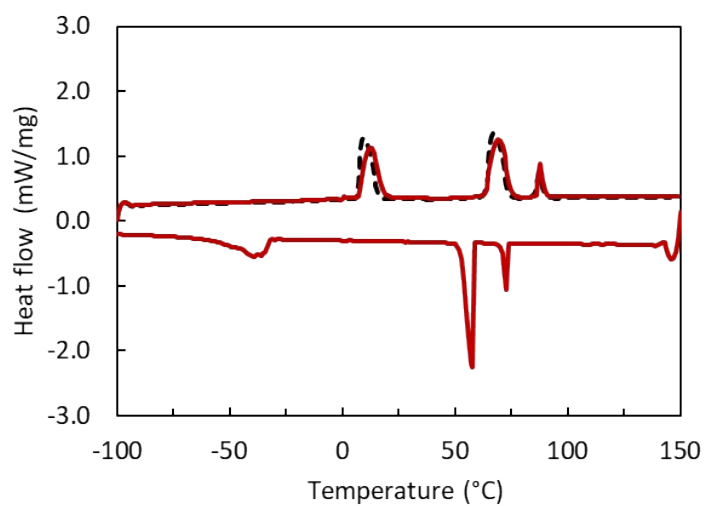


Figure S18. DSC curve of neat [HMG][FSI]. Scan rate: 10 K min<sup>-1</sup>.

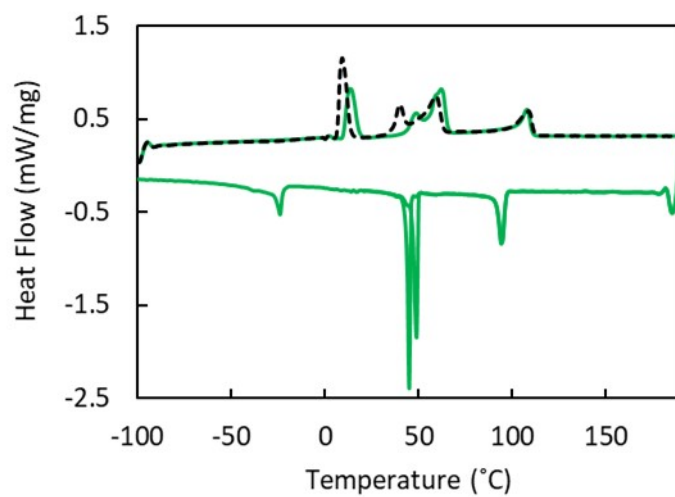


Figure S19. DSC curve of [HMG][FSI] + 5% NaTDI. Scan rate: 10 K min<sup>-1</sup>.

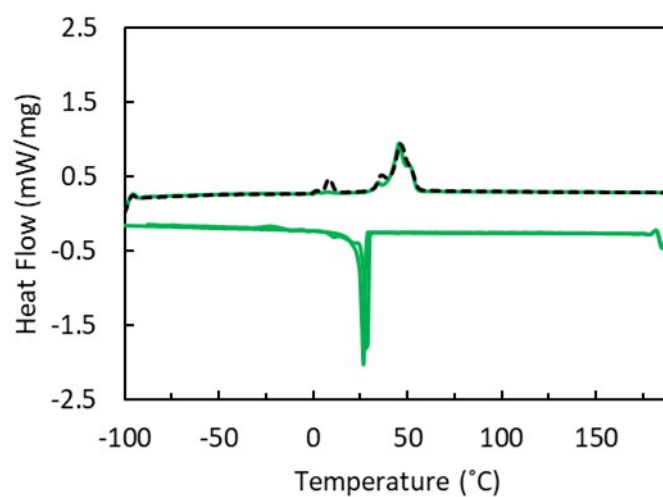


Figure S20. DSC curve of [HMG][FSI] + 10% NaTDI. Scan rate: 10 K min<sup>-1</sup>.

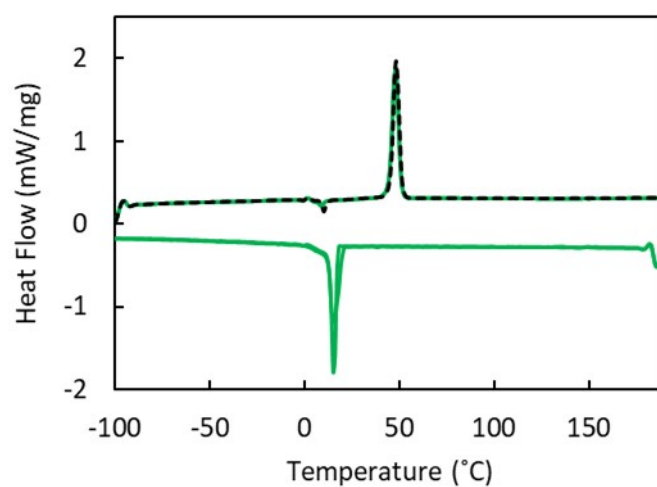


Figure S21. DSC curve of [HMG][FSI] + 15% NaTDI. Scan rate: 10 K min<sup>-1</sup>.

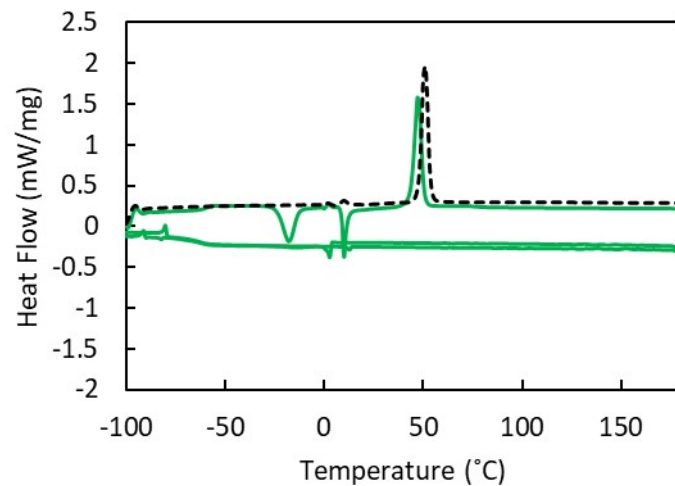


Figure S22. DSC curve of [HMG][FSI] + 20% NaTDI. Scan rate: 10 K min<sup>-1</sup>.

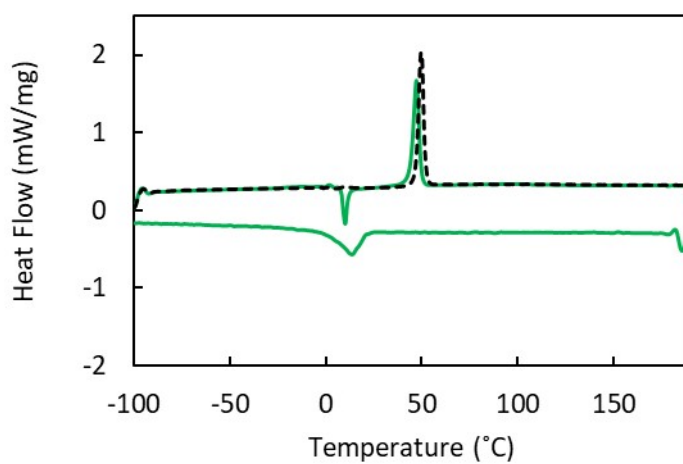


Figure S23. DSC curve of [HMG][FSI] + 25% NaTDI. Scan rate: 10 K min<sup>-1</sup>.

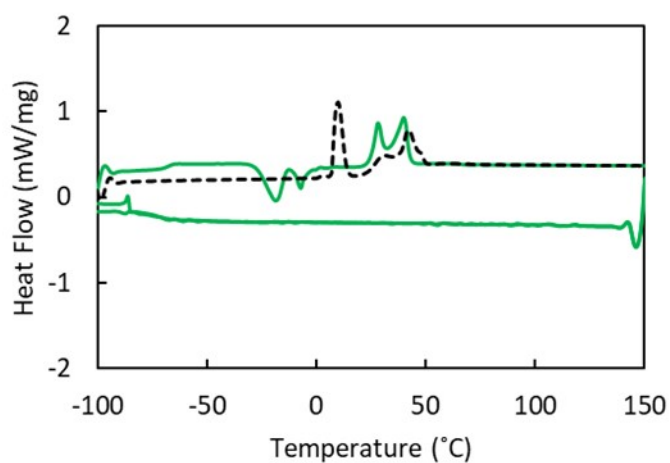


Figure S24. DSC curve of [HMG][FSI] + 30% NaTDI. Scan rate: 10 K min<sup>-1</sup>.

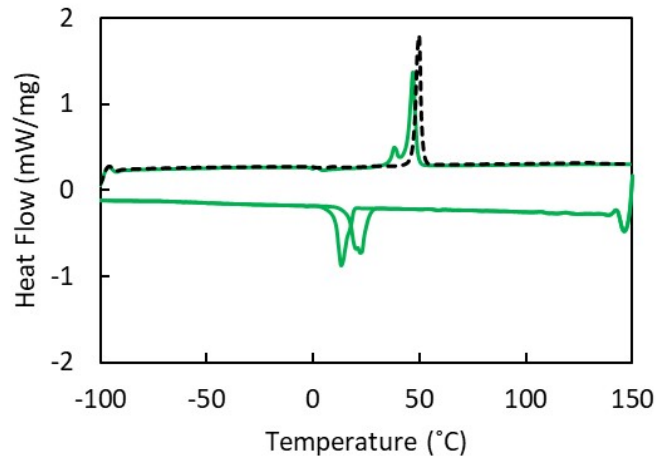


Figure S25. DSC curve of [HMG][FSI] + 40% NaTDI. Scan rate: 10 K min<sup>-1</sup>.

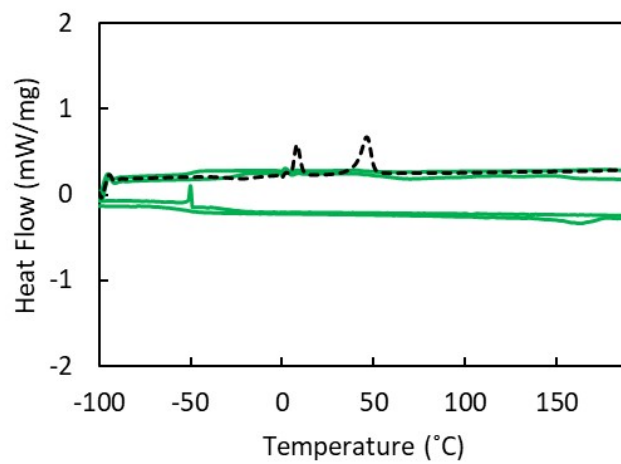


Figure S26. DSC curve of [HMG][FSI] + 50% NaTDI. Scan rate: 10 K min<sup>-1</sup>.

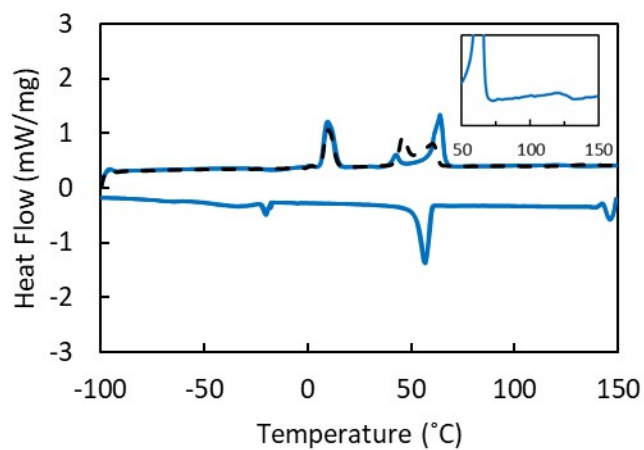


Figure S27. DSC curve of [HMG][FSI] + 10% NaTCM. Scan rate: 10 K min<sup>-1</sup>. Superpositioned graph displays zoomed in 50 - 150 °C range of 2<sup>nd</sup> heating cycle, demonstrating the melting transition.

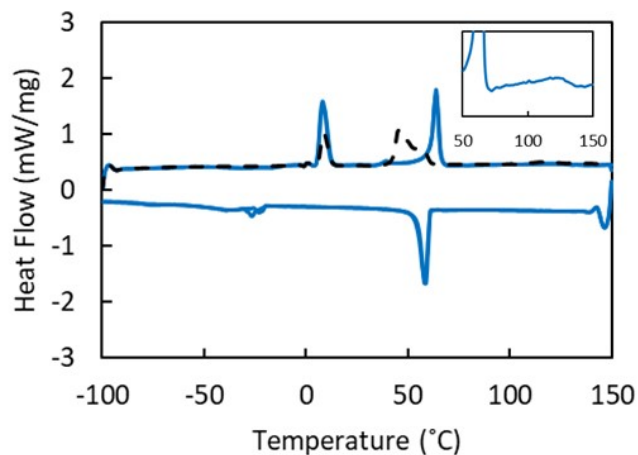


Figure S28. DSC curve of [HMG][FSI] + 20% NaTCM. Scan rate: 10 K min<sup>-1</sup>. Superpositioned graph displays zoomed in 50 - 150 °C range of 2<sup>nd</sup> heating cycle, demonstrating the melting transition.

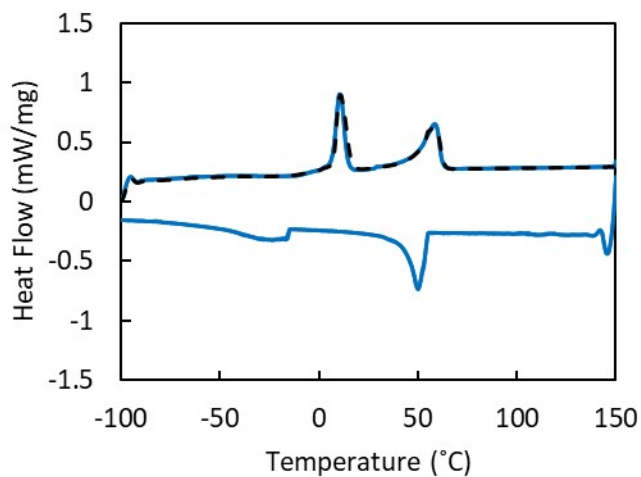


Figure S29. DSC curve of [HMG][FSI] + 30% NaTCM. Scan rate: 10 K min<sup>-1</sup>.

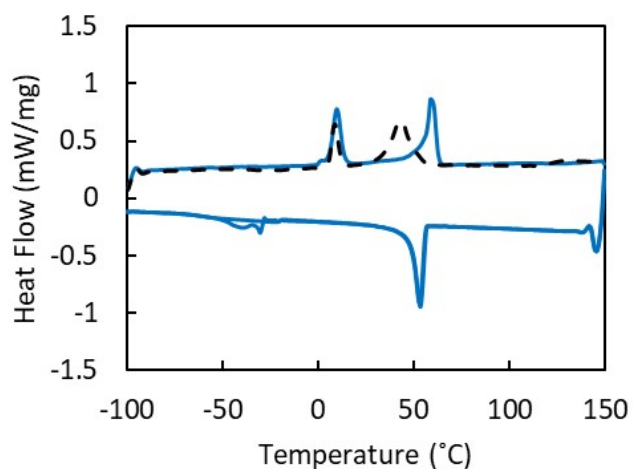


Figure S30. DSC curve of [HMG][FSI] + 40% NaTCM. Scan rate: 10 K min<sup>-1</sup>.

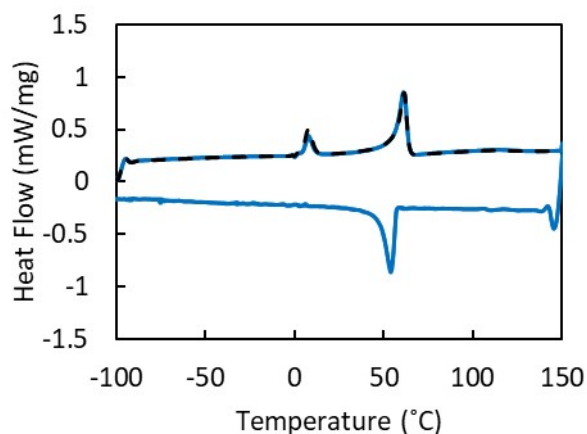


Figure S31. DSC curve of [HMG][FSI] + 50% NaTCM. Scan rate: 10 K min<sup>-1</sup>.

Table S4. Calculated  $E_a$  conductivity values for single and mixed-anion materials with temperature range of measurements used for calculations.

[HMG]-salt	Temperature range (°C)	Na-salt	Phase	$E_a$ (kJ/mol)	$E_a$ (eV)
[HMG][TDI]	30 - 90°C	10 mol% NaTDI	solid	112	1.16
	30 - 90°C	30 mol% NaTDI	solid	98	1.02
	30 - 90°C	50 mol% NaTDI	solid	22	0.23
[HMG][TCM]	60 - 90°C	10 mol% NaTCM	liquid	17	0.18
	60 - 90°C	20 mol% NaTCM	liquid	17	0.18
[HMG][FSI]	30 - 90°C	10 mol% NaTDI	liquid	24	0.25
	50 - 90°C	20 mol% NaTDI	liquid	22	0.23
	50 - 90°C	30 mol% NaTDI	liquid	20	0.21
[HMG][FSI]	60 - 90°C	10 mol% NaTCM	liquid	19	0.20
	60 - 90°C	20 mol% NaTCM	liquid	21	0.21
[C <sub>3</sub> mpyr][FSI] <sup>8</sup>	25 - 95°C	10 mol% NaFSI	liquid	21	0.22
	25 - 95°C	20 mol% NaFSI	liquid	24	0.24
	25 - 95°C	30 mol% NaFSI	liquid	29	0.30
	25 - 95°C	40 mol% NaFSI	liquid	33	0.34
	25 - 95°C	50 mol% NaFSI	liquid	38	0.40
	25 - 95°C	60 mol% NaFSI	liquid	47	0.49

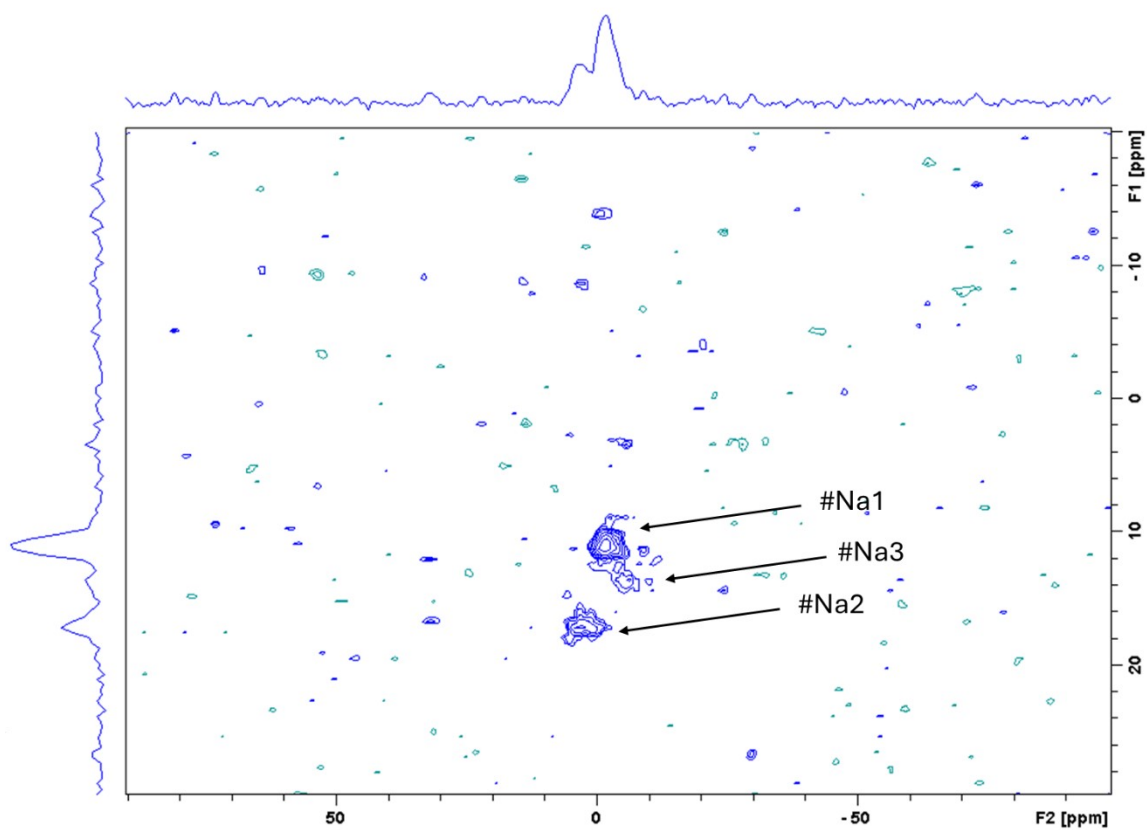


Figure S32.  $^{23}\text{Na}$  MQMAS NMR spectra obtained for [HMG][TDI] + 10 mol% NaTDI.

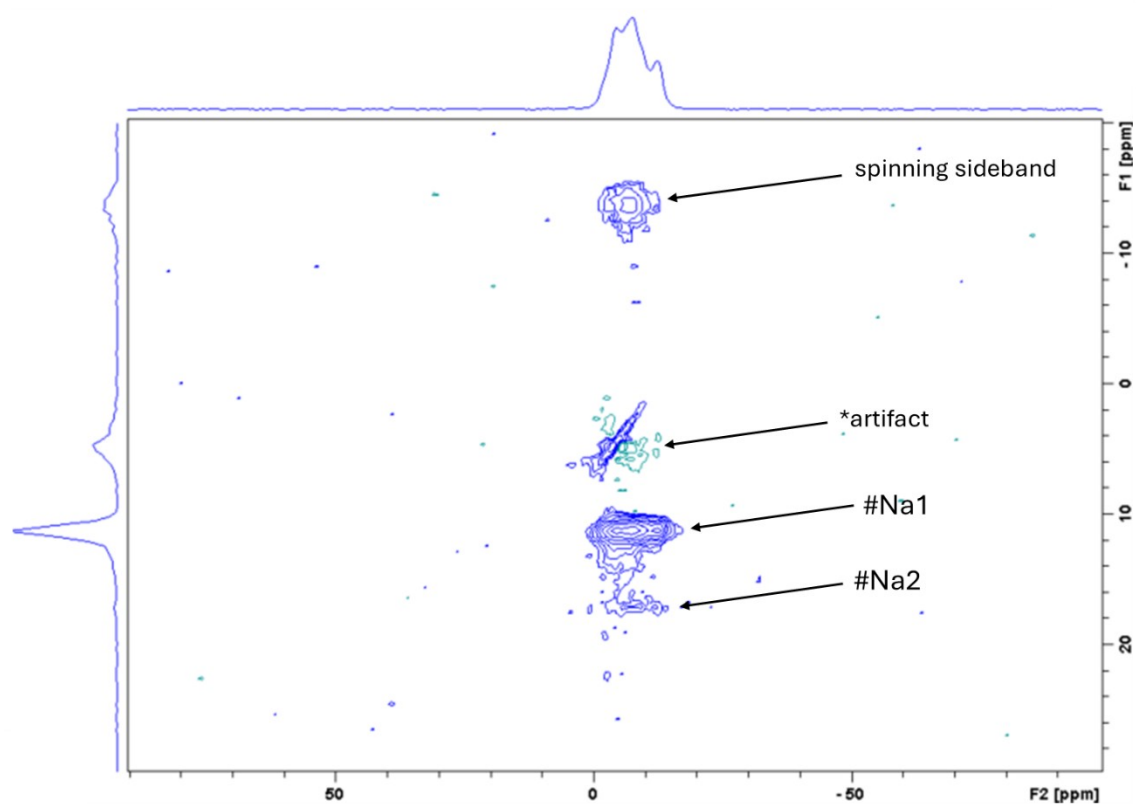


Figure S33.  $^{23}\text{Na}$  MQMAS NMR spectrum obtained for [HMG][TDI] + 50 mol% NaTDI.

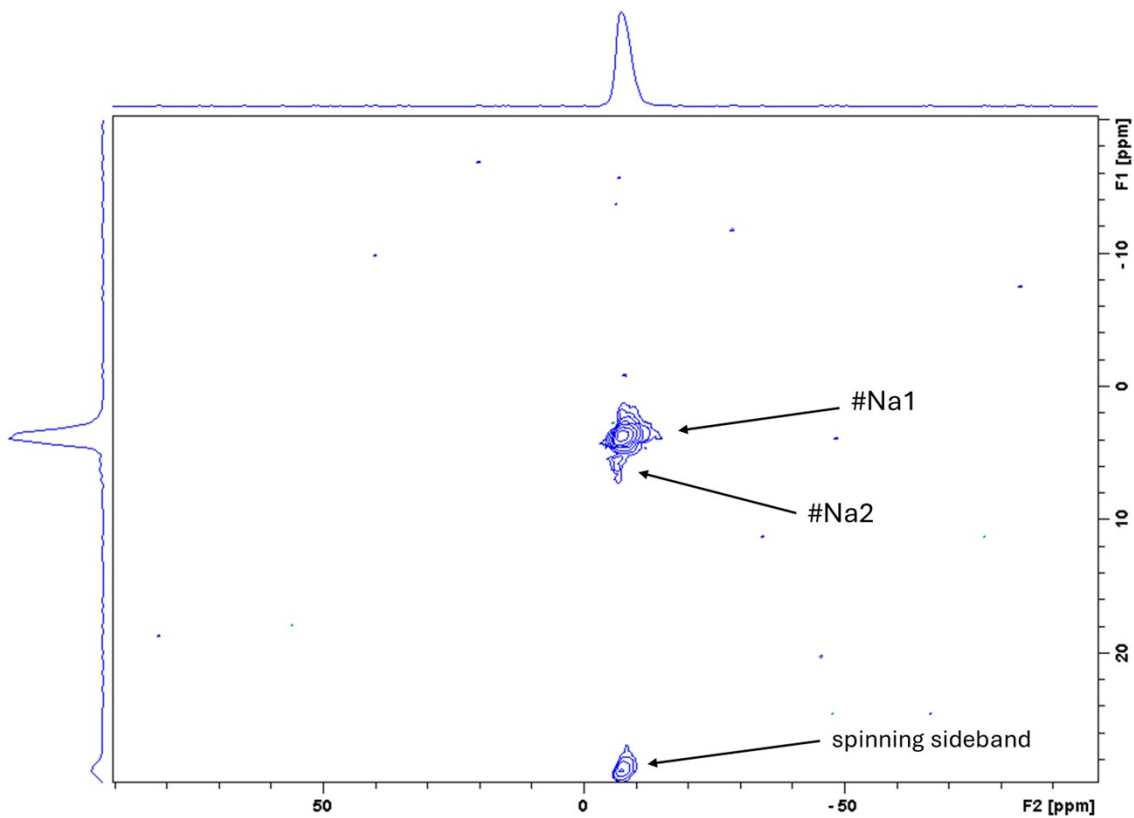


Figure S34.  $^{23}\text{Na}$  MQMAS NMR spectrum obtained for  $[\text{HMG}][\text{TCM}] + 20 \text{ mol\% NaTCM}$ .

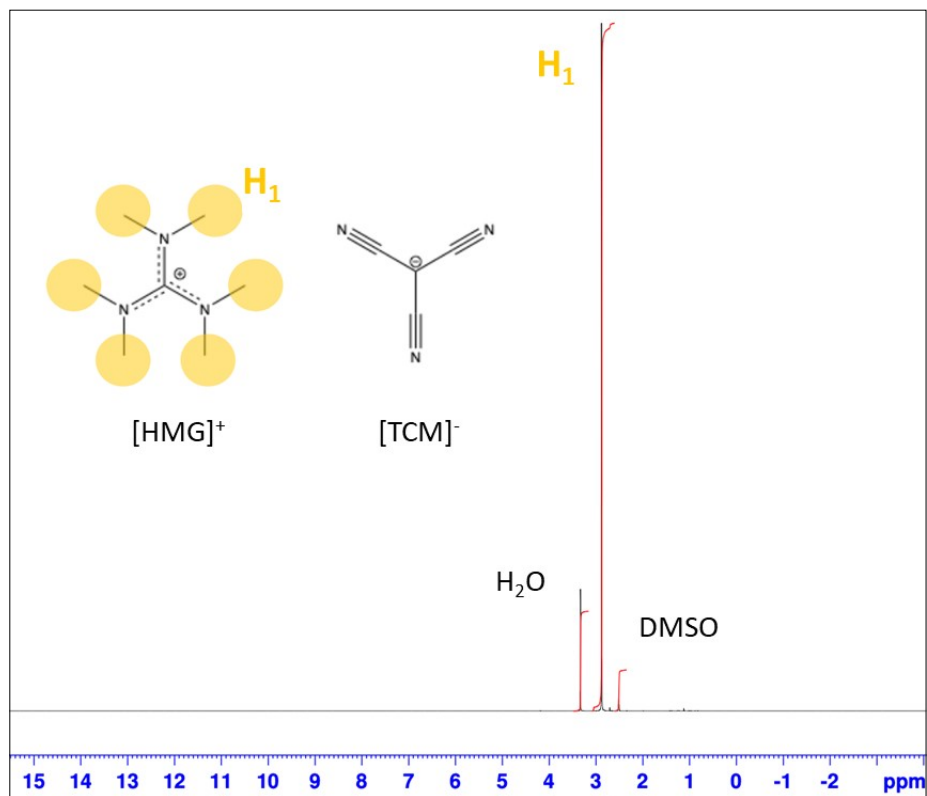


Figure S35.  $^1\text{H}$  NMR for hexamethylguanidinium tricyanomethane,  $[\text{HMG}][\text{TCM}]$

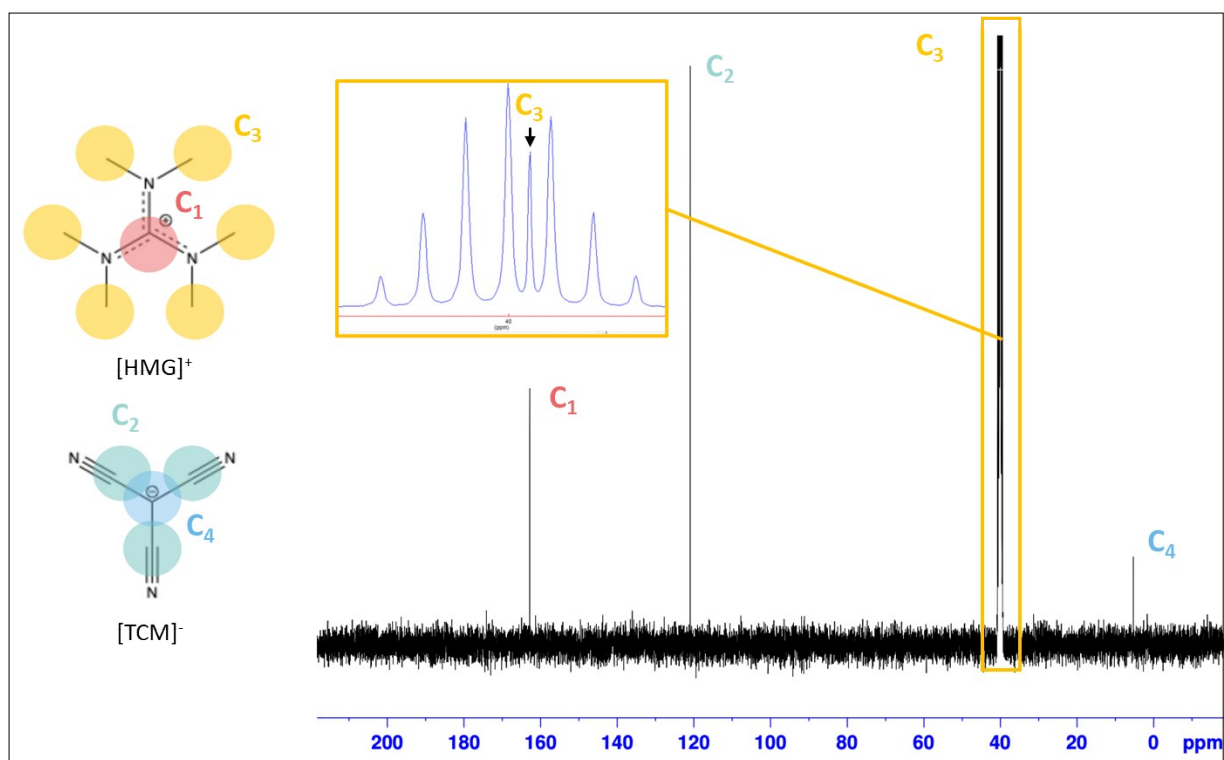


Figure S36. <sup>13</sup>C NMR for hexamethylguanidinium tricyanomethane, [HMG][TCM]

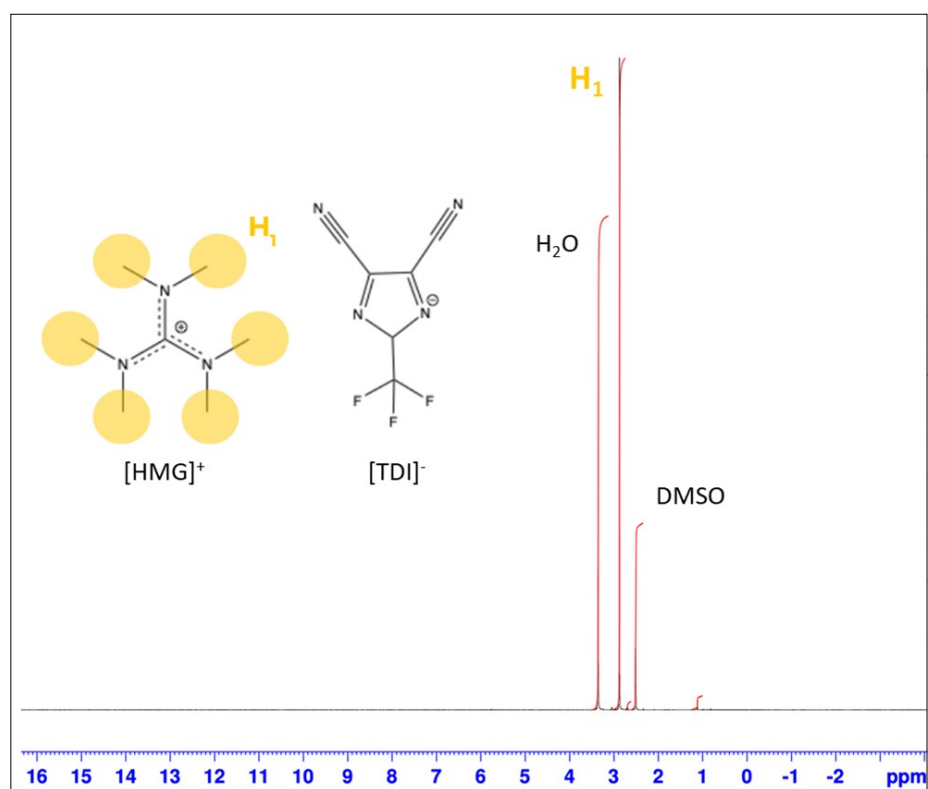


Figure S37. <sup>1</sup>H NMR for hexamethylguanidinium 4,5-dicyano-2-(trifluoromethyl)imidazolium, [HMG][TDI]

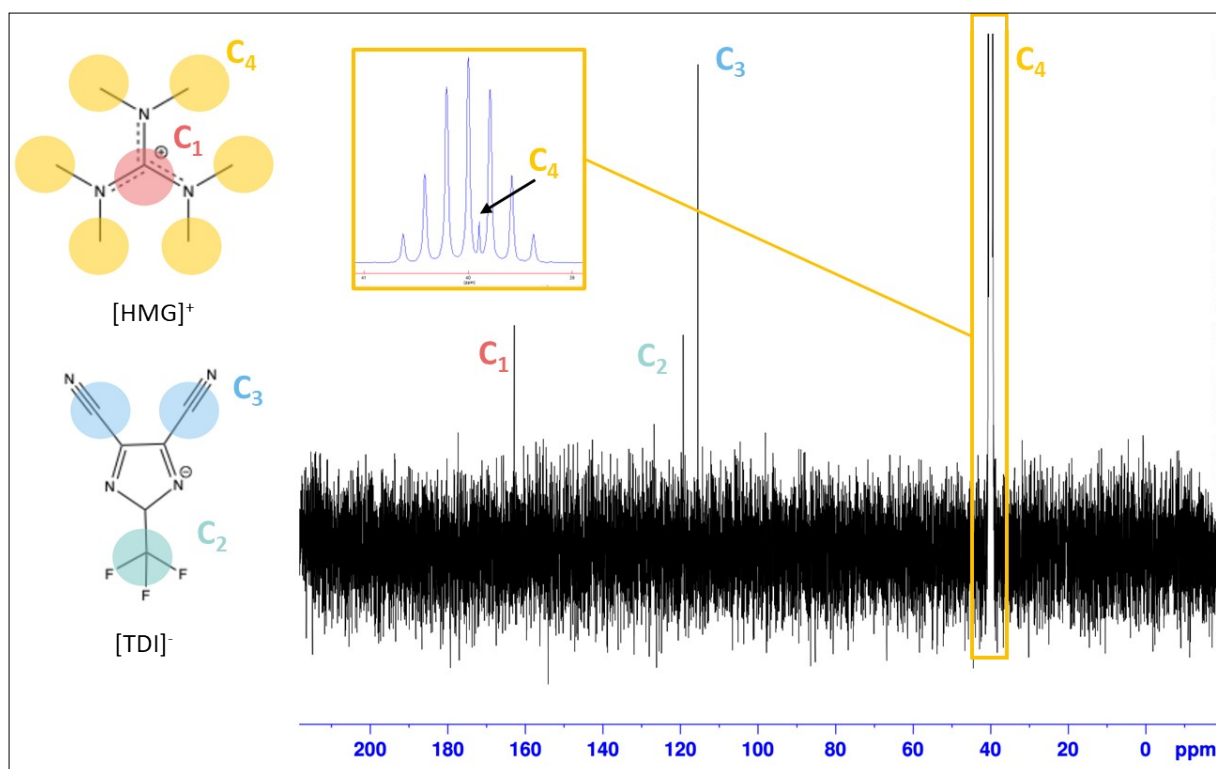


Figure S38.  $^{13}\text{C}$  NMR for hexamethylguanidinium 4,5-dicyano-2-(trifluoromethyl)imidazolium, [HMG][TDI]

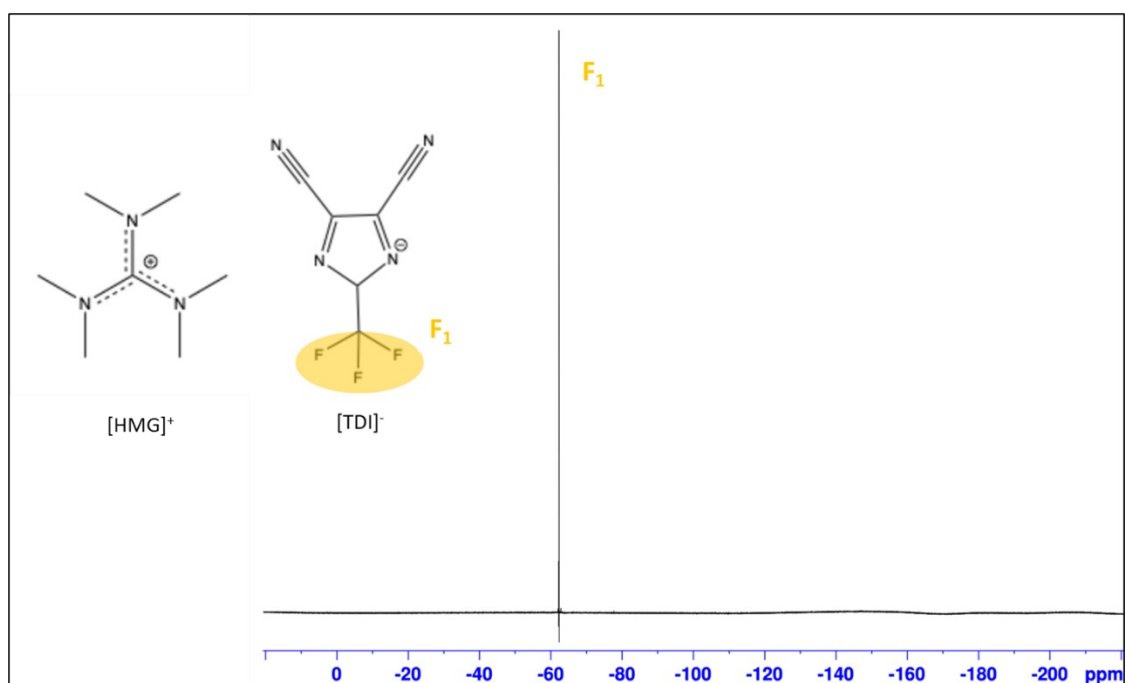


Figure S39.  $^{19}\text{F}$  NMR for hexamethylguanidinium 4,5-dicyano-2-(trifluoromethyl)imidazolium, [HMG][TDI]

## References:

- 1 C. Copeland, J. Ghosh, D. McAdam, B. Skelton, R. Stick and A. White, *Aust. J. Chem.*, 1988, **41**, 549.
- 2 R. Yunis, A. F. Hollenkamp, C. Forsyth, C. M. Doherty, D. Al-Masri and J. M. Pringle, *Phys. Chem. Chem. Phys.*, 2019, **21**, 12288–12300.
- 3 S. A. Forsyth, S. R. Batten, Q. Dai and D. R. MacFarlane, *Aust. J. Chem.*, 2004, **57**, 121.
- 4 V. L. Martins, A. J. R. Rennie, R. M. Torresi and P. J. Hall, *Phys. Chem. Chem. Phys.*, 2017, **19**, 16867–16874.
- 5 A. Sourjah, A. Mikus, C. M. Forsyth, W. Wieczorek, L. A. O'Dell and J. M. Pringle, *Chemistry A European J*, 2025, e202403681.
- 6 A. Ochel, D. Di Lecce, C. Wolff, G.-T. Kim, D. V. Carvalho and S. Passerini, *Electrochimica Acta*, 2017, **232**, 586–595.
- 7 L. Niedzicki, E. Karpierz, M. Zawadzki, M. Dranka, M. Kasprzyk, A. Zalewska, M. Marcinek, J. Zachara, U. Domańska and W. Wieczorek, *Phys. Chem. Chem. Phys.*, 2014, **16**, 11417–11425.
- 8 K. Matsumoto, Y. Okamoto, T. Nohira and R. Hagiwara, *J. Phys. Chem. C*, 2015, **119**, 7648–7655.